

The peculiar variable V838 Monocerotis

T. Kipper¹, V. G. Klochkova², K. Annuk¹, A. Hirv¹, I. Kolka¹, L. Leedjärv¹, A. Puss¹, P. Skoda³, and M. Slechta³

¹ Tartu Observatory, Tõravere 61602, Estonia

² Special Astrophysical Observatory, Nizhnij Arkhyz 369167, Russia
Isaac Newton Institute of Chile, SAO Branch
e-mail: valenta@sao.ru

³ Astronomical Institute CAS, Ondřejov 25165, Czech Republic
e-mail: skoda@pleione.asu.cas.cz

Received 6 June 2003 / Accepted 25 August 2003

Abstract. Spectroscopic observations of the peculiar variable V838 Mon during the period from the second light outburst until the fast dimming are presented. We describe high resolution ($R \approx 60\,000$) high S/N spectra obtained a day before the second light maximum and low resolution ($R \approx 6000$) spectra covering the whole period. The temporal run of intensities and radial velocities of various lines is presented. Using Na I D IS lines we determine the reddening distance of V838 Mon $d > 3.1$ kpc, and kinematic distance $d > 4$ kpc. We estimate that V838 Mon is slightly metal deficient but otherwise has a quite solar-like chemical composition except for enhanced abundances of Li, Ba and La.

Key words. stars: variables: general – stars: novae, cataclysmic variables – stars: individual: V838 Mon

1. Introduction

The peculiar object V838 Mon (RA $7^{\text{h}}04^{\text{m}}04^{\text{s}}.9$, Dec $-3^{\circ}50'51''.1$ (2000)) was photographically discovered by Brown (Brown et al. 2002) on January 06, 2002 when its brightness was $V \approx 10$. Brown noted that nothing appeared at the same position on December 22, 2001. The precise position of the object was measured by Oksanen & Solonen (Brown et al. 2002). Some authors have estimated the brightness of the progenitor. The results are quite different. Munari et al. (2002a) found using SERC plates $B = 16.10$ and $R_c = 15.30$. Kimeswenger et al. (2002) estimated $R = 14.56$ and $B = 15.87$ using SuperCOSMOS frames. Goranskii et al. (2002) found using the Digitized Sky Survey and SAI Crimean Station plates $B = 15.85 \pm 0.09$ and $R = 14.75 \pm 0.15$.

V838 Mon first showed a nova-like outburst with the usual decline, but this was followed by a second outburst after about one month, and then again after one month a third, somewhat weaker, one. After the third outburst the brightness declined quite rapidly and according to Henden (2002) reached $V = 16.04$ on August 22, 2002. The compiled light curve of V838 Mon is presented in Fig. 1. The dates of our spectral observations are also indicated in this figure. The available photometry of V838 Mon has been discussed by Munari et al. (2002a) and Kimeswenger et al. (2002). Here we present and discuss our spectroscopic observations.

2. Observations

A set of high resolution ($R \approx 60\,000$) spectra was obtained with the Nasmyth Echelle Spectrometer (Panchuk et al. 1999; Panchuk et al. 2002) of Russian 6 m telescope on February 04/05, 2002 (JD 2452310). The rapidly rotating A1V star HR 4687 was also exposed for reduction purposes. The spectra cover $\lambda\lambda 4610 \div 6060$ without any gaps. These spectra were reduced using the NOAO astronomical data analysis facility IRAF. The spectral orders were extracted using HR 4687 exposures. The continuum was placed by fitting low order functions through manually indicated points in every order. The spectrum of HR 4687 was used for determining the sensitivity function of orders. These high resolution spectra are discussed in the Sect. 3.2.

On the same night the low resolution ($R \approx 6000$) observations were started with the Cassegrain spectrograph of the Tartu Observatory 1.5 m telescope. The spectra were recorded with the cryogenically cooled CCD camera Orbis-1. This limited the wavelength coverage of a single exposure to about 400 Å. During various nights different numbers of exposures were obtained for the total wavelength region $\lambda\lambda 4699 \div 7000$ and $\lambda\lambda 8490 \div 8740$, mostly depending on weather conditions. The nights when at least one exposure was secured are indicated in Fig. 1. These spectra were reduced using the ESO data analysis package MIDAS. Sections 3.3–3.5 are based on these low resolution spectra. For the dates for which we have no spectra observed at the Tartu Observatory, we used for analysing the temporal changes of Si II $\lambda 6347$, Fe I $\lambda 6663$, and H α lines the

Send offprint requests to: T. Kipper, e-mail: tk@aa1.ee

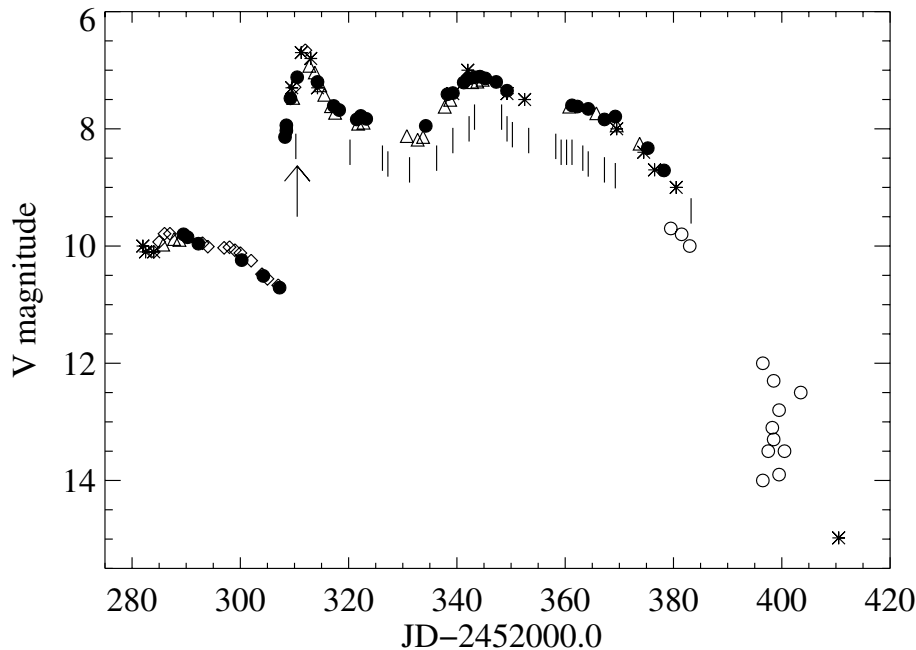


Fig. 1. V838 Mon lightcurve in V. Filled circles are the data from Kimeswenger et al. (2002), triangles and diamonds – Munari et al. (2002a). Some measurements, noted by asterisks, are supplemented from various sources (IAUC 7785, 7786, 7822, and 7889). The open circles are the quick-look data from AAVSO just for showing the fast weakening of the star. The last plotted point $V = 14.98$ was measured by Henden (2002). The arrow indicates the time of our high resolution spectral observation and the dates of the lower resolution spectra are indicated by the vertical dashes.

spectra obtained by Buil (2002) and spectra obtained with the Ondřejov 2 m telescope coude spectrograph ($R \approx 10\,000$). The Ondřejov coude spectra were reduced using IRAF.

Two additional spectra were obtained on March 08 and 18 with the Ondřejov 2 m telescope and echelle spectrograph HEROS ($R \approx 20\,000$). These spectra were reduced by the HEROS standard package written by O. Stahl in Heidelberg. These spectra were obtained in two channels – blue, covering $\lambda\lambda 3900 \div 5700$, and red, covering $\lambda\lambda 5800 \div 8300$. The red spectra of March 18 (JD 2452352) were used to estimate the chemical composition. The blue spectra are too noisy for that purpose.

3. Spectral evolution

3.1. Early spectra

Already the first spectra (January 8 and 9) obtained prior to our observations were not typical of Fe- or He/N-type classical novae early in their evolution (Wagner et al. 2002; Della Valle & Iijima 2002). The spectra cover $\lambda\lambda 3930\text{--}8560$ (Wagner et al. 2002) and $\lambda\lambda 4000\text{--}6800$ (Della Valle & Iijima 2002). These spectra showed numerous absorption lines (Fe II, O I, Ca II) and four prominent emission lines with P Cygni profiles. Three of these were identified with Ba II and the fourth was the Na I D doublet. $H\alpha$ was also weakly in emission. No absorption bands of TiO and C_2 were seen. These features allowed Della Valle & Iijima to suggest that the object could be a peculiar “slow” nova or a post-AGB star in the course of the He-flash.

The near infrared spectra (range 1.03–2.52 micrometers) obtained on January 12 by Geballe et al. (2002) showed shallow water bands at 1.4 and 1.9 micrometers, deep CO bands longward of 2.29 micrometers, hydrogen Brackett series lines and numerous strong metal lines (Mg I, Si I, Fe I) in absorption.

Many of the metal lines had P Cygni profiles indicating outflow velocities of several hundred km s^{-1} .

Zwitter & Munari (2002) obtained the first high resolution ($R \approx 18\,000$) spectra ($\lambda\lambda 4600\text{--}9300$) on January 26. They found that the spectrum resembles a heavily reddened cool K giant at heliocentric velocity $+53 \text{ km s}^{-1}$. Numerous absorption lines of Ca I, Ca II, Si I, Si II, Na I, Ni I, Y II, Zr II, C I, Cr I, Gd II, Fe I, and Ti I showed P Cygni profiles. They did not find Ba II lines.

The average terminal heliocentric velocity from the P Cygni absorption components was -458 km s^{-1} , with the line core at -252 km s^{-1} . The $H\alpha$ line showed narrow absorption at $+54 \text{ km s}^{-1}$ and weak emission at $+72 \text{ km s}^{-1}$. Interstellar Na I and K I lines were observed at velocities of $+37.1$ and $+64.9 \text{ km s}^{-1}$ and corresponded to $E(B - V) = 0.56$ and 0.24 , respectively. They also found a diffuse interstellar band (DIB) at $\lambda 8621$ with the equivalent width 0.29 \AA . From the reddening Zwitter & Munari suggested a distance of V838 Mon greater than 3 kpc.

Iijima & Della Valle (2002) also found in the spectra obtained a week later that numerous ionized metal lines (Fe II, Ti II, Cr II, Mg II, Si II) showed a P Cygni profile. These lines emerged between Feb. 1 and 2.

Morrison et al. (2002) obtained high dispersion ($R \approx 26\,000$) yellow region spectra about the same time as our spectra were observed. They found a few lines with P Cygni profiles belonging to Fe II, Na I, Si II, and $H\alpha$.

3.2. High resolution spectra obtained close to light maximum

As indicated in Fig. 1, our high resolution spectra were obtained about a day before V838 Mon reached its light maximum. Almost all metallic lines visible in our spectra showed P Cygni profiles. The lines identified belong to Na I, Mg I, Sc II, Ti II, Cr II, Fe I, Fe II, Sm II, Ba II. Some of the line profiles are

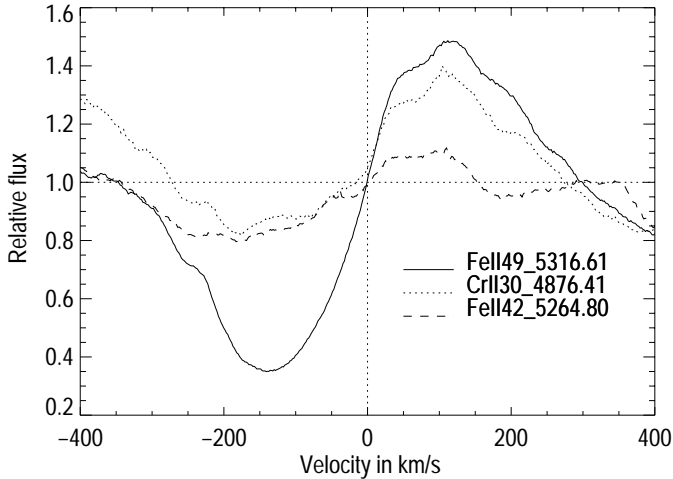


Fig. 2. The profiles of some lines in the spectrum of V838 Mon on February 04, 2002 (JD 2 452 310) on a velocity scale.

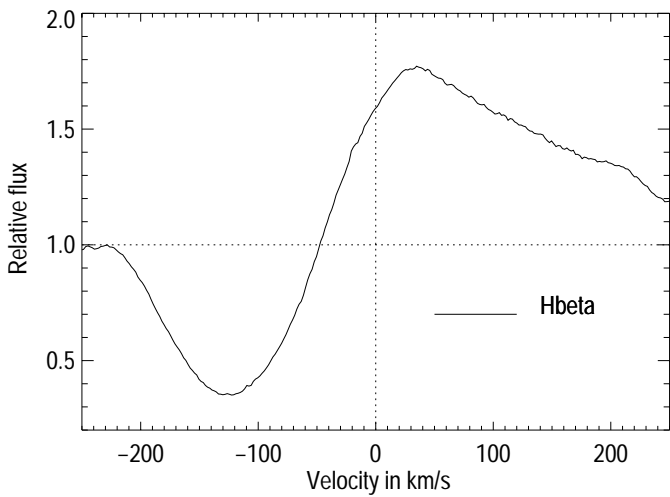


Fig. 3. Profile of the $H\beta$ line in V838 Mon on February 04, 2002 (JD 2 452 310) on a velocity scale.

illustrated in Figs. 2 and 3. Faint absorption lines ($R_c \approx 0.97$) of Fe I and Ca I were also found. Their identification is rather uncertain. Some of those faint Fe I lines also show P Cygni type emission components (Fig. 4).

3.2.1. Radial velocities

The metallic lines with P Cygni profiles have several components both in absorption and emission. The wavelengths of the components were determined by manually placing the cursor when using IRAF's task "splot". The mean heliocentric velocities of absorption components are -269 ± 6 and -182 ± 9 km s $^{-1}$. In the weaker lines additional components at velocities -121 ± 9 and -55 ± 13 km s $^{-1}$ could be found. In emission two components with heliocentric velocities $+25 \pm 5$ and $+93 \pm 4$ km s $^{-1}$ are visible. If these emission peaks are interpreted as belonging to approaching and receding parts of the expanding shell, the expansion velocity would be around 35 km s $^{-1}$ and the systemic velocity $+59 \pm 6$ km s $^{-1}$. For the faintest ($R_c \approx 0.97$) Fe I and Ca I lines only the absorption components at $+50 \pm 4$ km s $^{-1}$ are

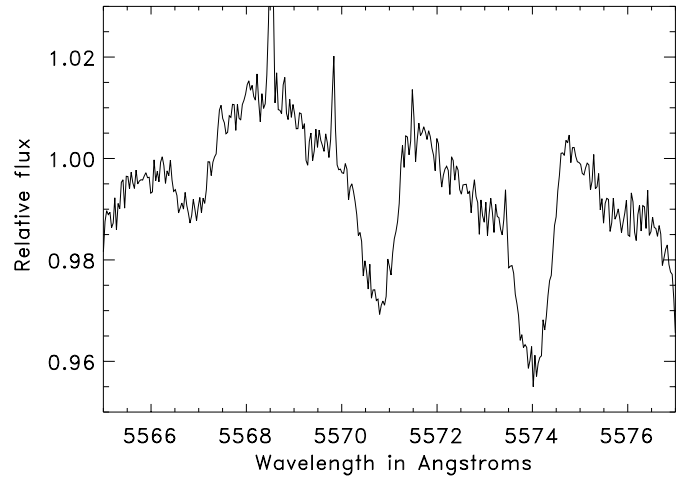


Fig. 4. Faint Fe I lines at 5565.71, 5569.63 and 5572.85 Å.

visible. For slightly stronger lines ($R_c \leq 0.96$) this is accompanied by the absorption at -50 ± 5 and emission at $+95 \pm 7$ km s $^{-1}$.

As noted before, Zwitter & Munari (2002) estimated systemic velocity $+53$ km s $^{-1}$ on January 26. Munari et al. (2002a) found for the same time using La II absorption lines the mean heliocentric velocity $+54.4$ km s $^{-1}$. In our spectra no La II lines are visible as stronger La II fall outside of our observed spectral region.

The terminal velocity derived from strong Fe II 42 lines is -388 km s $^{-1}$ and -240 km s $^{-1}$ from $H\beta$ line. These velocities are lower than those found by Munari et al. (2002a) from observations two weeks earlier. Munari et al. found that the reduction of terminal velocities continued also in February and March. These velocities are much lower than in classical novae. Only in the slowest classical nova HR Del and in RR Pic the absorption components of H I and metallic lines were blue-shifted by about -600 to -700 km s $^{-1}$ in the early stage and about -70 to -200 km s $^{-1}$ at the end of the pre-maximum stage (Iijima et al. 1998).

3.2.2. Na I D lines and the distance

The Na I D lines also show a P Cygni profile with three strong interstellar (IS) components (Fig. 11). The terminal velocity from D₂ line is -250 km s $^{-1}$. Three separate Gaussians could be fitted to the IS components. The results are given in Table 1. Without Gaussian decomposition the shorter wavelength IS components correspond to the heliocentric velocity $+36.1$ km s $^{-1}$. Our velocities are close to the ones found by Zwitter & Munari (2002) $+37.1$ and $+64.9$ km s $^{-1}$. Kolev et al. (2002) found velocities $+37.3$ and $+63.9$ km s $^{-1}$. They suggested that the bluer component could be of circumstellar origin together with unusually strong DIBs (see also Sect. 3.2.3).

Using the calibration of Munari & Zwitter (1997) we found the reddening from the equivalent widths of IS lines (Table 1). The total reddening is $E(B - V) = 0.49$ and the total visual extinction $A_V = 1.5$. This extinction corresponds to a distance of 3.1 kpc if the extinction maps by Neckel & Klare (1980) are used. The other estimates of $E(B - V)$ span from 0.7

Table 1. Heliocentric velocities, equivalent widths, and corresponding reddenings $E(B - V)$ of interstellar Na I D lines in V838 Mon spectra.

Line	V_r [km s ⁻¹]	W_λ [Å]	$E(B - V)$
D ₂	26.7 ± 0.5	0.26 ± 0.02	0.10
	45.0	0.47	0.27
	65.0	0.30	0.12
D ₁	28.2	0.28	
	44.0	0.31	
	63.5	0.35	

(Kimeswenger et al. 2002) to 0.9 (Munari et al. 2002b). The latter value was derived assuming that the apparent hot companion star (or just the star in the same position) is a genuine B3 dwarf. The distance to that star is then 10.5 kpc. V838 Mon is placed in a relatively low reddening region and the relevant field of the Neckel & Klare (1980) calibration is quite large and apparently overestimates the reddening towards V838 Mon. The dust distribution maps by Schlegel et al. (1998) allow us to determine the upper limit of $E(B - V) = 0.89$ in that direction. This coincides with the Munari et al. (2002b) value, therefore fixing the upper limit of the distance at 10.5 kpc.

In the Leiden/Dwingeloo HI survey (Hartmann & Burton 1997) in the direction of V838 Mon three complexes of clouds with the mean heliocentric velocities of 67.7, 42.8, and 27.1 km s⁻¹ (or 50.3, 25.3, and 9.7 km s⁻¹ relative to LSR) could be identified. These velocities are close to the ones found from the Na I D IS lines.

Assuming that the observed radial velocities reflect the Galaxy rotation and the peculiar velocities of the clouds do not exceed 7 km s⁻¹, the distances of these clouds would be 0.9 ± 0.7 kpc, 2.3 ± 0.9 kpc, and 5.7 ± 1.4 kpc. These estimates, however, being very crude, still allow us to place V838 Mon not much closer than 4 kpc. Wisniewski et al. (2003) used Na I D IS line radial velocities together with the velocity map of the outer Galaxy by Brand & Blitz (1993) and found 2.5 ± 0.3 kpc as the lower limit of the distance to V838 Mon. These kinematic distances are consistent with the distances estimated from the reddening. On the other hand, these distance estimates are in sharp disagreement with the ones found using the light echo expansion measurements. Munari et al. (2002a) estimated in this way the distance of 790 ± 30 pc and Kimeswenger et al. (2002) found the distance of 640 to 680 pc relying on the assumption of spherical geometry. However, Bond et al. (2002a) used imaging of the V838 Mon light echo in polarized light with the Hubble Space Telescope on May 20, 2002 and found the lower limit of the distance 2.5 kpc if the polarized ring was illuminated by the light emitted in the March 11 outburst. If that light was emitted on February 7, when the star was the brightest, the distance would be 3.6 kpc. The latest estimates from the light echo expansion by Bond et al. (2002b) give the distance between 3 and 7 kpc, again in the same range as the kinematic distances and the distances found from the interstellar reddening. Using the polarimetric imaging with HST Bond et al. (2003) even set the lower limit to the distance at 6 kpc.

Table 2. Observed wavelengths, heliocentric velocities, and equivalent widths of DIBs in the spectrum of V838 Mon, and corresponding reddenings $E(B - V)$. For the visual region DIBs the first column of $E(B - V)$ corresponds to Jenniskens & Désert (1994) calibration and the second to Josafatsson & Snow (1987) data. For $\lambda 8621$ DIB the calibration by Munari (1999) was used.

Wavelength	V_r [km s ⁻¹]	W_λ [Å]	$E(B - V)$	
5781.82	63 ± 2	0.73 ± 0.05	1.3	1.6
5798.43	64	0.21	1.6	1.6
5851.26	62	0.1:	2.1	1.3
8620.79 ¹		0.15	0.41	

¹ Not measured.

3.2.3. Diffuse interstellar bands

The spectra show also the presence of diffuse interstellar bands (DIB) at 5780.37, 5796.96, 5849.80 and 8620.79 Å (mean rest wavelengths from Galazutdinov et al. 2000). The observed DIB wavelengths, equivalent widths, and corresponding reddenings are given in Table 2. The reddenings are estimated from equivalent widths using the calibration data by Jenniskens & Désert (1994) and Josafatsson & Snow (1987). These reddenings turn out to be much larger than those obtained from Na I IS lines. However, the reddenings derived from the visual region DIBs should be considered very inaccurate as their extremely different strength ratios indicate (Krełowski & Schmidt 1997). The velocities, however, are close to the velocity of the most redshifted Na I D IS line velocity and also to the assumed systemic velocity. Therefore these DIBs do not originate from the same region as the blue IS components of the Na I D doublet as proposed by Kolev et al. (2002).

On our low resolution spectra a medium intensity DIB at $\lambda 8621$ is visible. Munari (1999) has shown that the equivalent width of this DIB correlates tightly with the reddening. Our estimate of $E(B - V)$ from this DIB is very close to the one from the Na I D IS lines.

3.3. Low resolution spectra

Our sequence of low resolution spectra of V838 Mon covers the period from 4th of February to 4th of April 2002 representing the brightness evolution from the rising branch of the second outburst to the beginning of the deep light weakening after the third outburst (Fig. 1).

The spectral evolution of V838 Mon after the second outburst is best characterized by the continuous decrease of excitation with a temporary increase during the third light maximum and possible expulsion of a new amount of material during the minimum between the second and third maxima. We have found that the intensity pattern of typical lines belonging to both neutral and ionized species has been remarkably correlated with the lightcurve in parallel to the main trend of dropping excitation. This trend is illustrated in Fig. 5 where the spectra in the H α region are depicted. The vertical shift of individual spectra in this figure is proportional to the time which

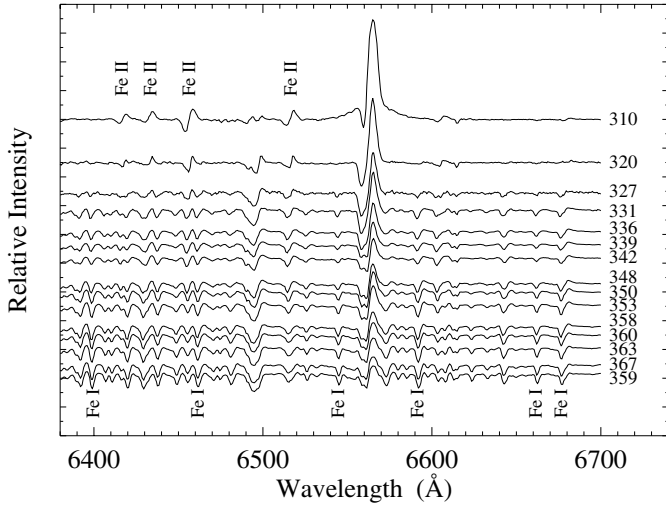


Fig. 5. The temporal change of the V838 Mon spectrum in the vicinity of the H α line. The vertical shift of the spectra is proportional to time. The time is indicated as JD–2 452 000. Note that not all the obtained spectra are depicted here in order to avoid crowding.

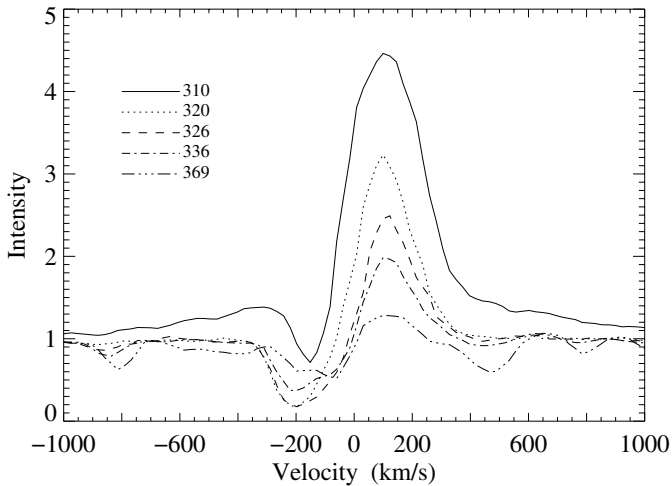


Fig. 6. Some representative profiles of H α line in the spectrum of V838 Mon on velocity scale. The observing time is indicated as JD–2 452 000.

runs downwards. One could clearly see the gradual weakening of Fe II and increase of Fe I lines. Also, the emission in Fe II and H α decreases rather fast.

Just before the second outburst, the H α line showed strong and very broad wings extending more than ± 1500 km s $^{-1}$ (Fig. 6). These wings disappeared 10 days later (JD 2 452 320). In the spectra obtained by Buil (2002) these wings are slightly visible until JD 2 452 318 (below we use for marking the dates shorter expressions used as tick labels in figures e.g. JD..318 instead of JD 2 452 318). According to Buil's observations the intensity of the broad wings changes together with the central intensity of the H α line (Fig. 7). Osiewała et al. (2003) have suggested Raman scattering of Ly β photons by neutral hydrogen as an explanation of these wings.

At the time when H α broad emission wings were visible, the absorption component had a radial velocity of about -180 km s $^{-1}$ and total width about 150 km s $^{-1}$. When

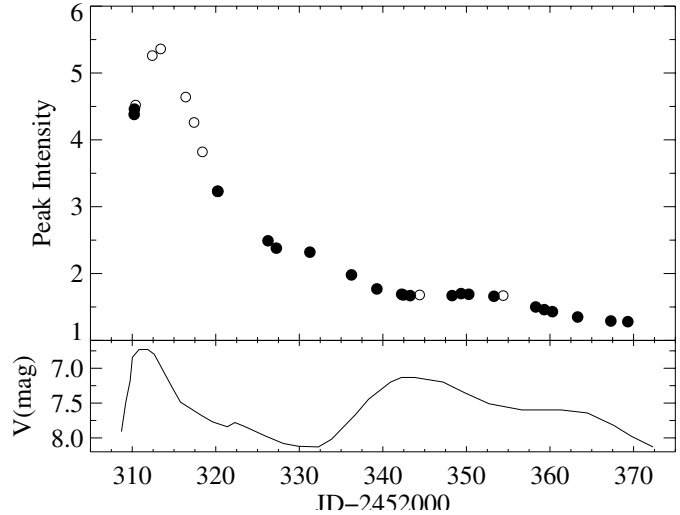


Fig. 7. The temporal change of H α intensity in V838 Mon spectrum starting with the second outburst. Filled circles indicate our observations, open circles are the observations by Buil (2002). For comparison the schematic lightcurve in V is given.

the broad wings disappeared, the absorption velocity increased to -200 km s $^{-1}$ and the width to 300 km s $^{-1}$. Starting from JD..326 a new absorption component starts to form and is clearly visible 5 days later at velocity -60 km s $^{-1}$. This is the time when the visual brightness of the star had its minimum between the second and third outburst. At the same time the H α emission was slightly stronger than on the neighbouring days. The radial velocity of the H α main absorption trough at -200 km s $^{-1}$ did not change during the whole following period covered by our observations, although the intensity of the trough was decreasing. In contrast to that, the originally developed P Cygni type profiles of ionized species (Si II, Fe II), while weakening, also decreases the blueshift of the absorption trough.

On JD..320 a local lightcurve bump starts to develop. This bump is not visible in *B*, but is slightly noticeable in *V*, and well developed in *I* (Bond et al. 2003).

Simultaneously with the H α absorption component at a radial velocity -60 km s $^{-1}$, Fe I lines start to strengthen (Fig. 8). Until that time Fe I absorption lines were extremely weak and the radial velocity estimates for the $\lambda 6663$ line in Fig. 8 are very uncertain but not in conflict with estimates from high resolution spectra for JD..310 (see Sect. 3.2.1). The new absorption component developed at larger blueshift than the disappearing one. During the periods of deepest absorption a few percent emission peak developed in Fe I $\lambda 6663$. Other Fe I lines behave similarly. The strengthening of Fe I lines is reversed during the third light maximum and continues when the star weakens again. During all that time the blueshift of Fe I lines decreases at a mean rate 1 km s $^{-1}$ d $^{-1}$. One of the best measured cases of the Fe I $\lambda 6546$ line is depicted in Fig. 9.

The intensity of the emission and absorption components of the low excitation Ba II $\lambda 6497$ line ($\epsilon_l = 0.6$ eV) increases considerably between JD..313 and JD..316. The absorption component continues to grow for several days after that, and then stays at nearly the same level until the end of our observations.

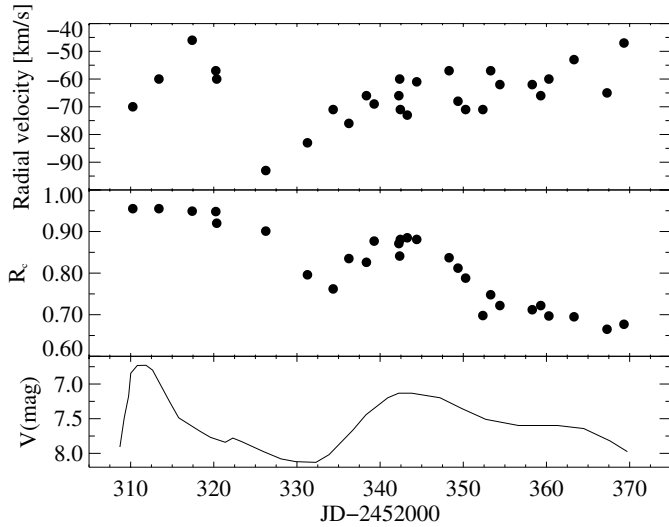


Fig. 8. The run of the residual intensities and corresponding radial velocities of absorption component of the Fe I $\lambda 6663$ line.

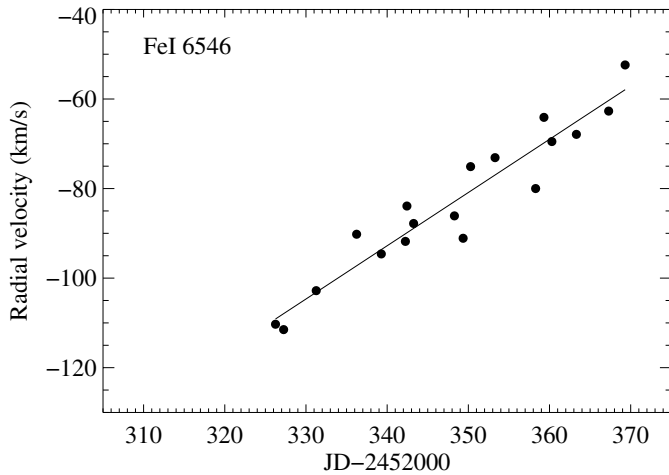


Fig. 9. The change with time of the radial velocity of the absorption component of Fe I $\lambda 6546.25$ line.

This means that a new layer of mass was expelled around JD 2452320. Further evidence supporting that suggestion is given in Fig. 10, where the temporal run of the residual intensity and the radial velocity of two absorption components of Si II $\lambda 6347$ line is presented. One of these components, which had its maximum strength slightly after the second light maximum, disappeared and a new one started to form. The velocity change of this new component is close to the Fe I line velocities. The line strength, however, changes in the opposite direction. This is what is expected if the line strength is mainly determined by excitation conditions.

The low excitation strong lines such as Na I D lines and Ca II $\lambda 8542$ behave somewhat differently – even at the end of March high terminal velocities up to -350 km s^{-1} were observed. Before the second light outburst these lines showed terminal velocities up to -500 km s^{-1} (Munari et al. 2002a; Kolev et al. 2002) but highly blueshifted wings of Na I D lines disappeared during several days before the second outburst. A possible explanation for that is that the sudden rise of colour

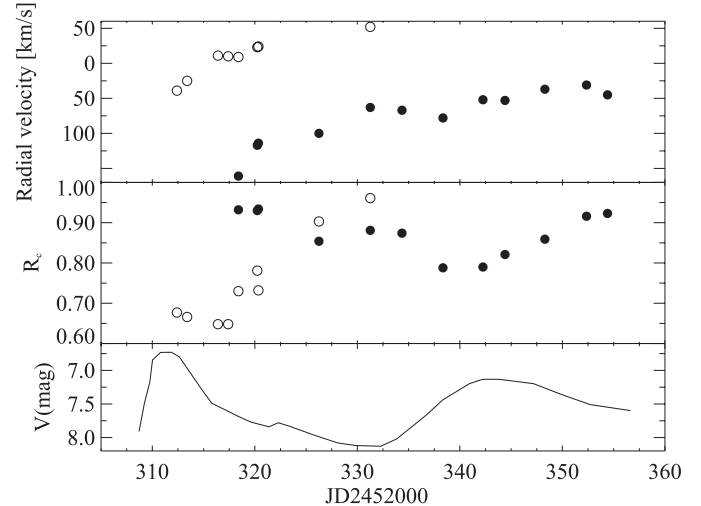


Fig. 10. The run of the residual intensities and corresponding radial velocities of two absorption components of Si II $\lambda 6347$ line. One component is plotted with open circles, another one with filled circles.

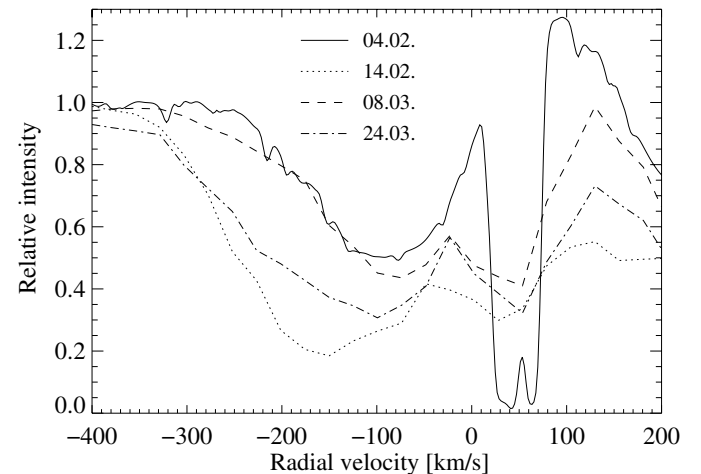


Fig. 11. Profiles of Na I D₂ line for various dates. Note, that at the light maxima on February, 04 and March, 08 the profiles are virtually identical. The spectral resolution of the Feb., 04 spectrum is much higher than for the other spectra.

temperature at the first moments of the second brightening caused much higher excitation in the whole volume of gas outflow. During the minimum between the second and third outbursts, Na I D lines develop stronger blue absorption line wings again. At the third outburst these wings disappeared again (Fig. 11).

3.4. Spectral classification

Munari et al. (2002a) have interpreted the broad-band colour variability of V838 Mon in terms of changing blackbody temperature having maxima at the peaks of lightcurve. This is in accord with our findings on spectral lines. We have made a crude quantitative estimate of the excitation temperature in the absorption line forming region by comparing our spectra of V838 Mon in the blue $\lambda\lambda 4600\text{--}5000$ and near-IR $\lambda\lambda 8500\text{--}8700$ regions with a set of standard spectra of supergiants ranging from A0 I to K0 I. These stars were observed

Table 3. Spectral classification of V838 Mon.

Date	Region	Sp	$T_{\text{eff}}(Sp)$	$T_{\text{eff}}(BB)$	$(B - V)$	$(B - V)_0$
2002						
04.02.	blue	A5	8610		1.1	0.09
07.02.				5200		
14.02.	blue	F5	6370		1.4	0.39
20.02.	blue	G0	5370	4150	1.9	0.75
25.02.	blue	G0–G5	4930–5370		2.0	0.90
02.03.	blue	G0	5370		1.85	0.75
05.03.	blue	F5–G0	5370–6370		1.70	0.75
05.03.	<i>n</i> – IR	G0–G4	4930–5370		1.70	0.75
08.03.	blue	F5–G0	5370–6370	4600	1.78	0.58
14.03.	<i>n</i> – IR	G4–G6	4930		1.86	1.08
24.03.	blue	G5	4930			
26.03.	<i>n</i> – IR	G6–G8	4700–4900			
02.04.	blue	>G5	<4900			
02.04.	<i>n</i> – IR	G8–K0	4550–4700			

Comparison stars:

HR 1040 – A0 Ia, HR 825 – A5 Ia, HD 7927 – F0 Ia,
 HD 10494 – F5 Ia, HD 18391 – G0 Ia, HD 47731 – G5 Ia,
 HD 6474 – G4 Ia, HD 63700 – G6 Ia, HD 12014 – K0 Ib.

at the Tartu Observatory in the blue region with the same resolution as V838 Mon. The near-IR reference spectra of comparable resolution were obtained from the database described by Cenarro et al. (2001). Our spectral classification results for different dates are presented in Table 3. In the fourth column of this Table the corresponding effective temperatures of supergiants (Drilling & Landolt 2000) are presented. In the fifth column the blackbody temperatures by Munari et al. (2002a) are given. The temperatures from the spectral classification are higher by up to 2000 K. It is possible to remove this difference by assuming larger IS reddening when reducing broad band data. Munari et al. (2002a) preferred $E(B - V) = 0.5$ but larger values up to 0.9 were later suggested by themselves (Munari et al. 2002b). The two last columns of Table 3 show the observed colours $(B - V)$ (Goranskii et al. 2002) and unreddened colours $(B - V)_0$ for the corresponding spectral class. The resulting colour excess is close to 1.0.

3.5. He I $\lambda 5876$ emission

On February, 14 (JD..320) we noticed that a few percent emission appeared in He I $\lambda 5876$ line. A closer inspection revealed that the weak emission line was present between 14th and 25th of February 2002. The emission peak of the line was blueshifted by 150 km s^{-1} with respect to other emission lines which had nearly constant heliocentric radial velocity around $+100 \text{ km s}^{-1}$. This line of highest excitation ($\epsilon_l = 20.87 \text{ eV}$) was probably not directly connected to the temperature rise at the beginning of the second outburst, otherwise it should have been visible already on JD..310. Combining our data with the similar ones by Wisniewski et al. (2003) we confirm that the He I $\lambda 5876$ line was absent up to JD..315. We tried to check the presence of He I $\lambda 6678$ line. This line is severely blended with an Fe I line. Up to JD..313 the blend behaved as

other neutral iron lines. Starting from JD..316 a clear blend of two lines appeared and the presence of extra emission was obvious. Later the intensity of the neutral iron lines started to grow and the contribution from He I could not be monitored. In summary, we are convinced that He I emission was present from Feb., 10 (JD..316) until the end of the month. The origin of these lines should be different from the other lines considered. One could suspect that they formed near another hotter star. The B3V companion found by Desidera & Munari (2002) could be such a star if it really is the companion to V838 Mon.

3.6. Chemical composition

In the spectra obtained in March the P Cygni emission components were significantly weakened and therefore there was some hope that the abundance analysis using spectrum synthesizing could be performed. The red echelle spectra obtained in Ondřejov on March 18, 2002 are of reasonable quality for that.

According to Munari et al. (2002a) the energy distribution in the continuum corresponded to 4600 K on March 08 and to somewhat lower temperature on March 18. If the mass of the star is around $1 M_{\odot}$ and the distance is 6 kpc, the absolute bolometric magnitude with this temperature (4500 K) will be $M_{\text{bol}} = -9.6$ and the surface gravity $\log g = -1.5$. With these parameters we started our experiments.

A small grid of atmospheric models with solar abundances was computed for temperatures $T_{\text{eff}} = 4500 \div 5500 \text{ K}$ and gravities $\log g = -0.5 \div -1.5$. The model atmospheres were computed with an improved version of the MARCS program (Gustafsson et al. 1975) which was modified in order to include molecular and metallic line opacities in an OS approximation.

Computed spectra with the starting temperature show a strong molecular (CN) spectrum which is not observed. This forced us to raise T_{eff} to 4750 K, assuming solar abundances of C and N and $\log g = -1.5$. This temperature is close to the mean of the colour temperature (Munari et al. 2002a) and the excitation temperature derived from spectral classification. To compute the CN spectrum we used the data from the SCAN-CN tape (Jørgensen & Larsson 1990). For metallic lines we used the line-list by Bell (1976) with some oscillator strengths corrected according to Thevenin (1989, 1990). The simultaneous fit of the weak and strong Fe I lines allows us to fix $\xi_t = 12 \pm 2 \text{ km s}^{-1}$. The large uncertainty here is due to the small number of strong lines. The abundances from lines stronger than $R_c \approx 0.5$ suffer from this uncertainty. The observed lines are much wider than the instrumental profile. We attribute this extra broadening to the macroturbulence of 75 km s^{-1} . The great width of the lines makes the blending large. We could not therefore use the many lines that are clearly present but hopelessly blended.

The use of the ionization equilibrium of iron allowed to confirm the surface gravity $\log g = -1.5 \pm 0.3$.

The resulting abundances are given in Table 4. We stress that the indicated uncertainties show only the differences in abundances found from different lines. The atmospheric parameters were not firmly established and the static LTE atmospheric models are very sketchy for this star, which on

Table 4. Abundances in V838 Mon on March, 18 2002.

El.	$\log \varepsilon(\text{El})_{\odot}$	$\log \varepsilon(\text{El})_{\text{V838Mon}}$	$[\text{El}/\text{Fe}]_{\text{V838Mon}}$
Li	3.31	3.8	0.9
Si	7.55	6.5 ± 0.2	-0.6
Ca	6.36	6.1 ± 0.3	0.2
Sc	3.17	2.9 ± 0.2	0.1
Ti	5.02	4.3 ± 0.3	-0.3
V	4.00	3.6 ± 0.4	-0.1
Cr	5.67	5.0 ± 0.2	-0.3
Mn	5.39	4.9 ± 0.2	-0.1
Fe	7.50	7.1 ± 0.3	
Co	4.92	4.3 ± 0.3	-0.2
Ni	6.25	5.7 ± 0.3	-0.2
Y	2.24	1.8 ± 0.2	0
Ba	2.13	2.5 ± 0.3	0.7
La	1.17	1.5 ± 0.4	0.7

March, 18 still showed P Cygni-type lines – clear indicators of mass outflow. Therefore these abundances should be considered only as very crude estimates.

From Table 4 one finds that the abundances of most elements are slightly less than the solar ones, $[\text{Fe}/\text{H}] = -0.4 \pm 0.3$. At the same time the lithium $\log \varepsilon(\text{Li}) = 3.8$, barium $\log \varepsilon(\text{Ba}) = 2.5$, and lanthanum $\log \varepsilon(\text{La}) = 1.5$ abundances are clearly enhanced. The abundances of Li and Ba are found from strong lines assuming $\xi_t = 12 \text{ km s}^{-1}$. With higher microturbulent velocity these overabundances are less. These abundances do not resemble the ones found in the “late He-flash” objects V4334 Sgr and FG Sge. This is an argument for not including V838 Mon in that type of object.

4. Discussion

Several scenarios have been proposed to explain the outburst of V838 Mon. The spectral evolution and mainly the absence of any nebular phase excludes the simplest scenario of classical nova. The nondetection of X-ray luminosity a year after the outburst with Chandra (Orio et al. 2003) is also strong evidence against nova-like thermonuclear runaway as a mechanism for the outburst.

The scenario of V838 Mon being a post-AGB object having a late helium flash was also discussed (Munari et al. 2002a) and rejected, mainly due to too fast evolution and the lack of strong carbon overabundance. The abundances found by us also rule out this model.

Two stars, V4332 Sgr in the Galaxy and a red variable in Andromeda galaxy (RV M31), were found to behave similarly to V838 Mon (Munari et al. 2002a; Kimeswenger et al. 2002). Kimeswenger et al. rule out RV M31 as a possible twin to V838 Mon on the basis that V838 Mon had the maximum luminosity much lower than RV M31. In the present paper we offer some arguments favouring the large distance for V838 Mon, and therefore it could have been as luminous as RV M31 which peaked at $M_{\text{bol}} = -9.95$ (Rich et al. 1989). If the distance of V838 Mon is greater than 6 kpc its absolute bolometric magnitude peaked at $M_{\text{bol}} = -9.6$.

In both cases (RV M31 and V4332 Sgr) there is no good explanation. For RV M31 Iben & Tutukov (1992) proposed a model where such a cold outburst of a short period CV is possible. But this would then lead to the complete destruction of the WD. In case of RV M31 at least two outbursts have been recorded (Sharov 1990). Sharov, however, later retracted his claim due to the low quality of the photographic material used (Sharov 1993). In the case of V838 Mon there have been previous outbursts which left the circumstellar envelope visible in the light echo. The nondetection of X-rays is also an argument against this scenario in the case of V838 Mon.

Soker & Tylanda (2003) proposed a scenario of merging of two main sequence stars of masses 1.5 and about $0.5 M_{\odot}$. This kind of merging also destroys the star and therefore is not applicable for recurrent outbursts. But they also suggest the merger of a zero-age horizontal branch star with a low mass main sequence star. Then the dust-halo illuminated by light-echo is a result of earlier high mass loss on RGB. However, in his recent study of the light echo of V838 Mon, Tylanda (2004) found that the light echo is of interstellar origin rather than produced by dust generated by mass loss in the past. If nature produces one of the merging scenarios, V838 Mon should be a triple system. The progenitor was estimated to be a hot $B \approx 15.9$ star (Munari et al. 2002a; Kimeswenger et al. 2002; Goranskii et al. 2002). After the outburst faded, this star is still there (Munari et al. 2002b). Although there is the possibility that this hot star lies in the same direction but farther away than V838 Mon, the brief existence of emission in the He I $\lambda 5876$ line seems to support the idea of physically bound multiple star.

Acknowledgements. The financial support to this work was provided by Estonian Science Foundation grant 5003. This study was also supported by grant 205/02/0445 of Grant Agency of the Czech Republic and by project 02-02-16085a of the Russian Foundation for Basic Research. We thank the referee, J. Landstreet, for the detailed and constructive remarks.

References

- Bell, R. 1976, private communication
- Bond, H. E., Panagia, N., & Sparks, W. B. 2002a, IAU Circ., 7914, 1
- Bond, H. E., Henden, A., Panagia, N., et al. 2002b, BAAS, 34, N4
- Bond, H. E., Henden, A., Levay, et al. 2003, Nature, 422, 405
- Brand, J., & Blitz, L. 1993, A&A, 275, 67
- Brown, N. J., Waagen, E. O., Scovill, C., et al. 2002, IAU Circ., 7785, 1
- Buil, C. 2002, <http://www.astrosurf.com/buil/us/nmon>
- Cenarro, A. J., Cardiel, N., Gorgas, J., et al. 2001, MNRAS, 326, 959
- Della Valle, M., & Iijima, T. 2002, IAU Circ., 7786, 1
- Desidera, S., & Munari, U. 2002, IAU Circ., 7982, 1
- Drilling, J. S., & Landolt, A. U. 2000, in Allen’s Astrophys. Quantities, ed. A.N. Cox (AIP Press Springer), 381
- Galazutdinov, G. A., Musaev, F. A., Krełowski, J., & Walker, G. A. H. 2000, PASP, 112, 648
- Geballe, T. R., Eyres, S. P. S., Evans, A., & Tyne, V. H. 2002, IAU Circ., 7796, 1
- Goranskii, V. P., Kusakin, A. V., Metlova, N. V., et al. 2002, Astron. Lett., 28, 691
- Gustafsson, B., Bell, R. A., Eriksson, K., & Norlund, Å. 1975, A&A, 42, 407

- Hartmann, L., & Burton, W. B. 1997, *Atlas of Galactic Neutral Hydrogen* (Cambridge Univ. Press), 10+236 pp
- Henden, A. 2002, *IAU Circ.*, 7598
- Iben, I. Jr., & Tutukov, A. V. 1992, *ApJ*, 389, 369
- Iijima, T., Rosino, L., & Della Valle, M. 1998, *A&A*, 338, 1006
- Iijima, T., & Della Valle, M. 2002, *IAU Circ.*, 7822, 1
- Jenniskens, P., & Désert, F.-X. 1994, *A&AS*, 106, 39
- Josafatsson, K., & Snow, T. P. 1987, *ApJ*, 319, 436
- Jørgensen, U. G., & Larsson, M. 1990, *A&A*, 238, 424
- Kimeswenger, S., Lederle, C., Schmeja, S., & Armsdorfer, B. 2002, *MNRAS*, 336, 43
- Kammerer, A., Garcia, J., Shida, R. Y., et al. 2002, *IAU Circ.*, 7822, 2
- Kiyota, S. 2002, *IAU Circ.*, 7786, 2
- Kolev, D., Mikołajewski, M., Tomov, T., et al. 2002, *Collected Papers, Physics* (Shumen, Bulgaria: Shumen University Press), 147
- Krelowski, J., & Schmidt, M. 1997, *ApJ*, 477, 209
- Kurucz, R. L. 1993, *CDROM13*
- Morrison, N. D., Bjorkman, S., & Miroshnichenko, A. 2002, *IAU Circ.*, 7829, 2
- Munari, U., & Zwitter, T. 1997, *A&A*, 318, 269
- Munari, U. 1999, *Baltic Astron.*, 8, 73
- Munari, U., Henden, A., Kiyota, S., et al. 2002a, *A&A*, 389, L51
- Munari, U., Desidera, S., & Henden, A. 2002b, *IAU Circ.*, 8005, 1
- Neckel, T. A., & Klare, G. 1980, *A&AS*, 42, 251
- Orio, M., Starrfield, S. G., & Tepedenlegliou, E. 2003, *IAU Circ.*, 8110
- Osiwala, J. P., Mikołajewski, M., Tomov, T., et al. 2003, *The Double Outburst of the Unique Object V838 Mon*, in *Symbiotic Stars Probing Stellar Evolution*, ed. R. L. M. Corradi, J. Mikołajewska, & T. J. Mahoney, *ASP Conf. Ser.*, 303, in press
- Panchuk, V. E., Klochkova, V. G., & Najdenov, I. D. 1999, *Preprint Special Astrophys. Obs.*, 135
- Panchuk, V. E., Piskunov, N. E., Klochkova, V. G., et al. 2002, *Preprint Special Astrophys. Obs.*, 169
- Rich, R. M., Mould, J., & Picard, A. 1989, *ApJ*, 341, L51
- Schlegel, D. J., Finkbeiner, D. P., & Davis, M. 1998, *ApJ*, 500, 525
- Sharov, A. S. 1990, *Astron. Lett.*, 16, 85
- Sharov, A. S. 1993, *Astron. Lett.*, 19, 33
- Soker, N., & Tylenda, R. 2003, *ApJ*, 582, L105
- Thevenin, F. 1989, *A&AS*, 77, 137
- Thevenin, F. 1990, *A&AS*, 82, 179
- Tylenda, R. 2004, *A&A*, 414, 223
- Wagner, R. M., Halpern, J. P., & Hackson, M. 2002, *IAU Circ.*, 7785, 2
- Wisniewski, J. P., Morrison, N. D., Bjorkman, K. S., et al. 2003, *ApJ*, 588, 486
- Zwitter, T., & Munari, U. 2002, *IAU Circ.*, 7812, 2